Dalton Transactions

ROYAL SOCIETY OF CHEMISTRY

PAPER

View Article Online
View Journal | View Issue

Cite this: *Dalton Trans.*, 2025, **54**, 16754

A spin-state switchable MOF-based film for visual DMSO vapor sensing

Yuwei Shen,[a] Soraya Bouras,[a] Latévi Max Lawson Daku,[b] Christian Serre[a] and Antoine Tissot *[a,c]

Received 24th September 2025,
Accepted 15th October 2025

DOI: 10.1039/d5dt02285a

rsc.li/dalton

The design of new colorimetric sensors for the detection of volatile organic compounds (VOCs) is of high interest due to the health issues they can induce. In this study, we report the fabrication of a film composed of the spin crossover complex $[Fe(Sal_2trien)]NO_3$ embedded within metal–organic framework nanocrystals. This composite material demonstrates a selective and reversible colorimetric response to dimethyl sulfoxide (DMSO) vapor exposure at room temperature, which is attributed to a spin state switching from high-spin (HS) to low-spin (LS) of the Fe(III) centers upon DMSO adsorption (down to 15 ppm_V). This work highlights the potential of integrating spin crossover complexes into MOFs to develop colorimetric and reusable VOC vapor sensors.

Introduction

Volatile organic compounds (VOCs) are hazardous volatile molecules responsible for many health issues worldwide.[1] The development of cheap, easy-to-handle and reliable sensors for these compounds is therefore of fundamental interest. Currently, many VOC sensors rely on conductivity measurements or quartz microbalances but these systems often lack selectivity and enable only total VOC (TVOC) quantification, which corresponds to the sum of all VOCs present in the air without identification of the individual components.[2,3] On the other hand, accurate assessment of all the components present in the air can be performed thanks to advanced analytical methods such as gas chromatography and mass spectrometry, but these techniques are expensive and not easily transportable. Optical sensing of VOCs is promising for the design of easy-to-handle sensors, as the readout can be performed with the naked eye or with cheap devices such as CCD cameras. The modulation of the optical properties of a sensor can occur through a change of color, refractive index or light emission in the case of luminescent solids.[4]

Ordered porous solids are particularly appealing for the design of optical VOC sensors, as they may combine optically switchable sites with selective sorption of target analytes.[5,6] Metal–organic frameworks (MOFs) are a class of crystalline micro- or meso-porous hybrid crystalline solids that present appealing features for sensing applications such as a large scope of structural features and possible functionalization combined with sensitive and selective vapor sorption features.[7] For example, luminescent MOFs based on optically active cations (mainly lanthanides) or organic linkers have been widely explored for the sensing of ions or organic molecules.[8,9] Several MOFs can also undergo a color change upon guest sorption, based on the coordination of the analyte to an accessible metal site or on supramolecular interactions between the analyte and the MOF backbone. However, most of the existing studies have been performed in the liquid phase and the investigation of their switching in the presence of vapors remains scarce.[10,11]

As an alternative strategy for the design of colorimetric sensors, researchers are beginning to explore the development of switchable porous solids based on the assembly of diamagnetic large pore MOFs with spin crossover complexes.[12,13] Indeed, spin crossover compounds are known to switch between the low spin (LS) and high spin (HS) states under several external stimuli such as temperature, light and pressure.[14] Moreover, a slight modification of their supramolecular environment can also induce a spin state change, for example, in the presence of vapors.[15] This spin state switching is accompanied by a modification of most physical properties of the compound, particularly its color. Based on this concept, we recently evidenced that loading spin crossover complexes in preformed chemically stable MOFs can lead to chemoswitchable solids that are sensitive to vapors of water, alcohols, formaldehyde and formic acid, even if the hybrid solids do not undergo noticeable thermal spin crossover.[16,17] On the other hand, some of us reported the design of a porous switchable

[a]*Institut des Matériaux Poreux de Paris, UMR 8004 CNRS, Ecole Normale Supérieure, ESPCI Paris, PSL University, 75005 Paris, France.*
E-mail: antoine.tissot@ens.psl.eu
[b]*Department of Physical Chemistry, University of Geneva, 1211 Geneva, Switzerland*
[c]*Institut de Chimie Moléculaire et des Matériaux d'Orsay, CNRS, Université Paris-Saclay, 91400 Orsay, France*

compound based on the loading of the model $Fe^{III}(sal_2trien)^+$ spin crossover complex in MOF-808(Zr), a benchmark Zr tricarboxylate MOF exhibiting 18 Å large pores.[18] The compound presents an abrupt thermal spin transition close to room temperature with a 15 K wide thermal hysteresis, regardless of the MOF particle size and the amount of complex loaded. It is therefore very promising for the design of a chemosensor, as both LS and HS states are close in energy at room temperature and therefore, a small stimulus might induce a spin state switching. Here, we present the shaping of the $Fe(Sal_2trien)NO_3$⊂MOF-808 compound into films of optical quality and the investigation of their switching properties in the presence of VOC vapors.

Results and discussion

Two strategies can be adopted to fabricate SCO⊂MOF-808 films: developing SCO⊂MOF nanoparticle suspensions or encapsulating the SCO complex into a pre-synthesized MOF-808 film. However, the first strategy might lead to the leaching of the SCO complex when dispersing the MOF particles in a solvent to process them as films. Therefore, we adopted the post-encapsulation strategy to integrate the SCO complex into a MOF-808 film, which was prepared *via* spin coating. In order to prepare a MOF-808 film, 35 nm MOF-808 NPs were first synthesized according to our previously published procedure (Fig. S2).[19] The wet nanoparticles were dispersed in ethanol at two concentrations: 6 mg mL^{-1} and 35 mg mL^{-1}. The colloidal stability of the resulting suspensions was investigated by a combination of dynamic light scattering and zeta potential measurements (Fig. S3). A colloidal particle size of around 90 nm was obtained at the lowest concentration, associated with a positive zeta potential value of above 20 mV, indicating the high colloidal stability of this suspension. At the highest concentration, only a slight increase in the particle size (up to 100 nm) and in the polydispersity index was observed, suggesting that the colloidal stability remains reasonable. Therefore, films were prepared using the spin coating technique by depositing a 30 mg mL^{-1} suspension onto a transparent glass slide in rotation at 1000 rpm. In each deposition, 100 μL of liquid was injected in order to guarantee the complete coverage of the substrate. Multiple depositions were performed to adjust the film thickness between 1 and 1.5 μm in order to evaluate if the film thickness influences its switching behavior.

With a 3-layer deposition, a transparent film presenting limited light scattering was obtained (Fig. S4a), which allowed investigation of its optical properties in the visible range using an optical absorption spectrometer. Although few cracks were observed due to the absence of a binder to increase the mechanical strength of the films after drying, the films presented satisfactory mechanical stability to be handled and used as a colorimetric sensor. Fig. S4c shows a SEM image of the cross-section of the film deposited on a Si wafer, evidencing that the film is homogeneous on the mm scale with an average thickness of 1 ± 0.2 μm. Higher resolution SEM indicated that the nanoparticles are tightly packed (Fig. S4d), which may explain the mechanical properties of the films. With a 5-layer deposition process, a thicker film (around 1.5 ± 0.3 μm) with similar mechanical and optical properties was obtained (Fig. 1 and Fig. S5).

Similar to that for the MOF-808 powder,[18] the films were then loaded with $Fe^{III}(Sal_2trien)NO_3$ by impregnation of the film in a solution of the complex in dichloromethane, followed by a washing step using the same solvent. UV-visible spectroscopy evidenced that the films exhibit an identical red-brown color to the powdered sample, associated with the LMCT transition of the HS complex at 520 nm (see Fig. 1 and Fig. S6, S7). The Fe : Zr ratio in the film was investigated by SEM-EDX analysis (Fig. S6) and the results are consistent with those obtained for the powdered sample. A slight decrease in the loading was observed for the thicker film, which may be related to the dense packing of MOF nanocrystals within the film, which hinders the diffusion of the complex into it.

As previously reported, $Fe(Sal_2trien)^+$ complexes present a solvatochromic behavior in solution at room temperature associated with a spin state switching.[20] This solvent dependence is attributed to the interactions through H-bonding between the solvating molecules and protons on the secondary amine of the trien backbone that are prone to stabilize the LS state. Consequently, $Fe(Sal_2trien)^+$ complexes are mainly HS in most organic solvents (HS fraction >0.7), while the LS state is more stabilized in DMSO (HS fraction of 0.5; see Fig. S8, S9 and Table S1 for characterization of the solutions by UV-visible spectroscopy and Evans ^{1}H NMR).

In order to explore the sensing response of $Fe(Sal_2trien)NO_3$⊂MOF-808 films towards different VOC vapors, a film was exposed to saturated vapors in a sealed container without any activation treatment (*e.g.* heat or vacuum). Before exposure, the pristine film presented a predominant HS (500 nm) absorption band, with a shoulder at 630 nm corresponding to LS species, in line with an almost exclusive population of the HS state (Fig. S10). Vapors of methanol, acetonitrile and toluene, which represent model vapors of polar protic, polar aprotic and nonpolar VOCs, did not induce any major changes in the optical spectra. In contrast, after exposure to DMSO, the color of the film turned dark purple with a significant reduction in absorbance at 500 nm and a corresponding increase in absorption at 630 nm. This evolution of the absorbance spectrum indicates stabilization of the LS state in the presence of DMSO vapors, in agreement with both the behavior of the complex in solution and the magnetic measurements performed on $Fe(Sal_2trien)NO_3$⊂MOF-808 powder loaded with vapors. Indeed, these measurements evidenced that at RT, the dry compound is predominantly HS, the hydrated compound presents an intermediate spin state, and the DMSO-loaded sample is mainly LS (Fig. S11).

In order to probe the interactions between the SCO complex, the DMSO adsorbed molecules and the MOF-808 backbone, well-tempered metadynamics (WT-MTD) and Born–Oppenheimer molecular dynamics (BOMD) simulations were

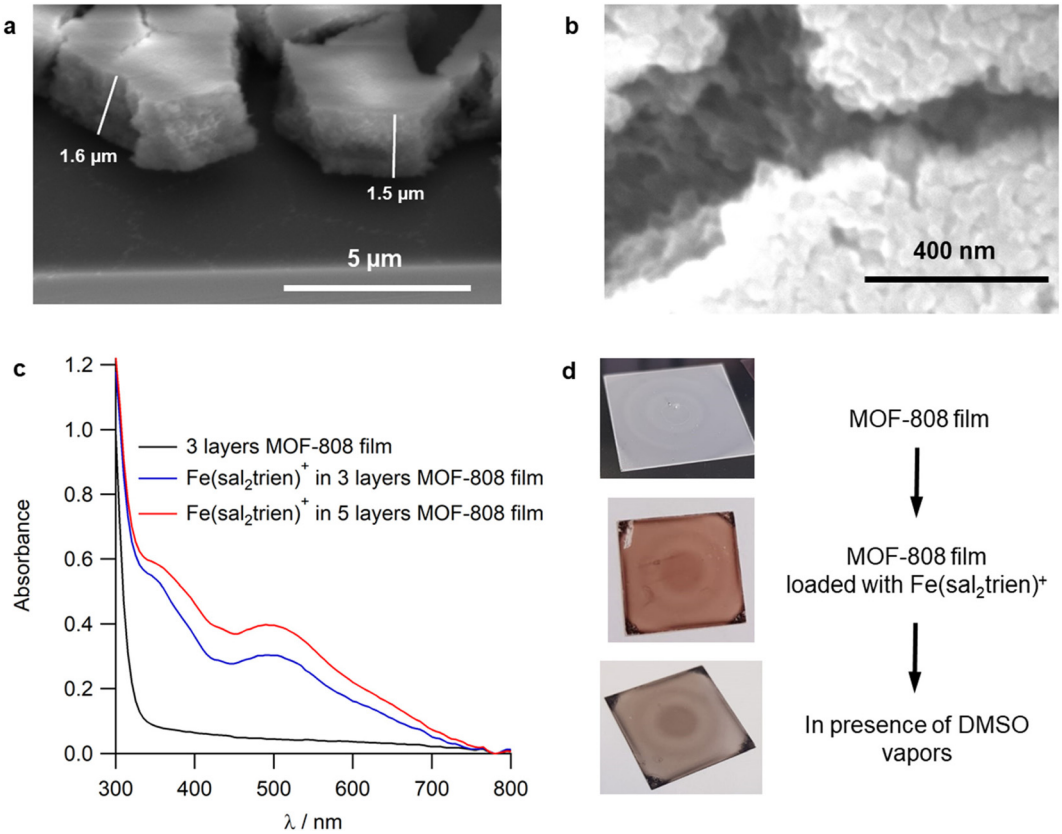

Fig. 1 (a) SEM image of the cross-section of a 5-layer deposition film deposited on a Si wafer. A factor of cos(45°) has been applied to the length measurement to correct the effect of the projection. (b) SEM images of the surface of a 5-layer deposition film. (c) Optical absorption spectra of the pristine film and the films prepared with different parameters after loading. (d) Optical image of a 5-layer deposition of a MOF-808 film, of a Fe(Sal_2trien)NO_3⊂MOF-808 film and of a Fe(Sal_2trien)NO_3⊂MOF-808 film in the presence of DMSO vapors (films deposited on a 25 mm square piece of glass).

performed with the tight-binding GFN-*x*TB method on a model system based on one complex loaded in the MOF-808 large pore. At first, the WT-MTD simulation was applied to determine the most favorable locations of $Ga^{III}(sal_2trien)^+$ in MOF-808 in the presence of DMSO molecules at T = 320 K, using as collective variables the Cartesian coordinates of Ga^{III} (see the SI for computational details; note that Ga^{III} was used instead of Fe^{III} at this stage (i) to allow faster calculations using a diamagnetic cation (closed-shell system) and (ii) also because of the similar ionic radii of HS Fe^{III} and Ga^{III}). Fig. S12 shows the reconstructed free energy surface (FES) $F(T = 320\ K; x_{Ga}, y_{Ga}, z_{Ga})$, evidencing that the complex is preferentially located close to the walls of the cavities of MOF-808, as previously reported when the complex is encapsulated in the absence of solvent.[18]

The (BOMD) simulations were then performed at T = 320 K with the $Fe^{III}(sal_2trien)^+$ complex in both LS and HS states (see the SI for computational details). Fig. 2 presents the spatial distribution functions of the O, S and C atoms of the DMSO molecules located in the close vicinity of the complex. They evidence that these molecules are engaged in the N–H···O hydrogen bonds with the amine groups of the ligand. The radial distribution functions $g(r)$ of the O, S and C atoms of DMSO with respect to the N_{amine} atoms of the complex (Fig. 2) further evidence that each amine group is engaged in a strong N–H···O hydrogen bond with one DMSO molecule. Therefore, the simulations strongly support the existence of a strong interaction between DMSO and the complex through H-bonding, which likely enhances the ligand field strength and therefore induces the stabilization of the LS state in the presence of DMSO.

Owing to the selective spin state switching of the Fe(Sal_2trien)$^+$ complexes in Fe(Sal_2trien)NO_3⊂MOF-808 in the presence of DMSO vapors, we then investigated the colorimetric switching of the films using a home-made *in situ* measurement chamber. Indeed, given that DMSO is considered potentially toxic, its monitoring in air could be of high relevance.[21,22] A 1.5 µm thick film was thus placed in the *in situ* measurement chamber to get an insight into the kinetics of its response when exposed to VOC vapors (see the SI for details of the setup). Prior to the measurements, the film was activated at 100 °C to remove absorbed water and traces of the loading solvent (DCM) from the pores. The absorbance of the activated film in the visible region mainly presents an absorption band at 500 nm, indicating that the complexes are in the HS state (Fig. 3). Afterwards, the film was exposed to a relatively high concentration (68 ppm_v) of DMSO vapor (N_2 carrier

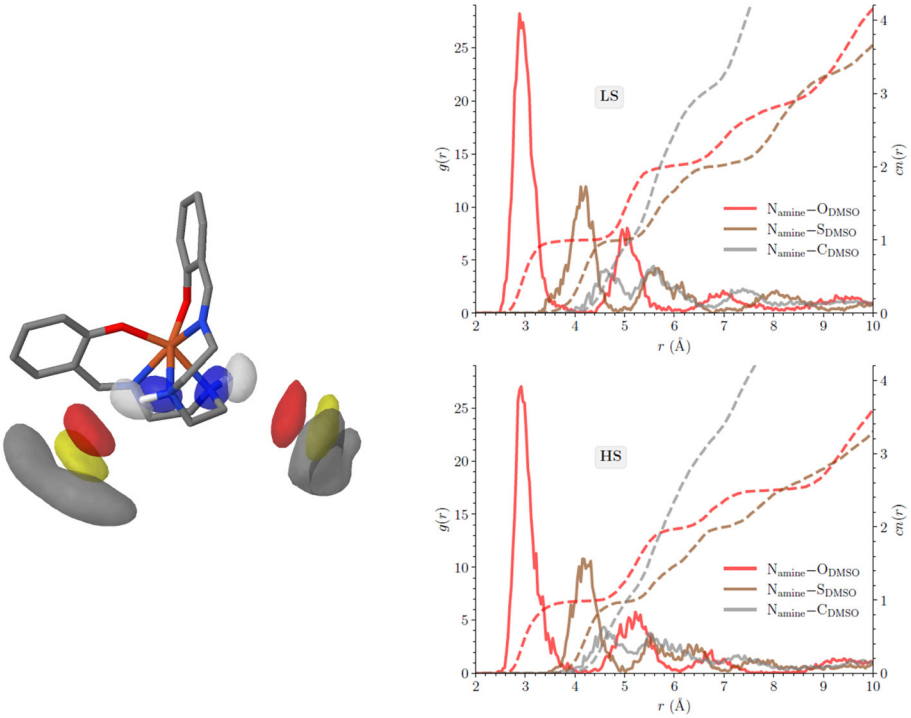

Fig. 2 (left) View of the spatial distribution functions of the O (red), S (yellow) and C (gray) atoms of the two DMSO molecules engaged in the N–H···O hydrogen bonds with the amine groups of the ligand. The spatial distribution functions of the H (white) and N (blue) atoms of the amine groups are also shown. All H atoms except those of the amine groups are hidden for the sake of clarity; (right) 'Solvation structure' of the N atoms of the amine groups (N_{amine}) for the Fe(III) complex in the LS (top) and in the HS (bottom) state: radial distribution functions $g(r)$ of the O, S and C atoms of DMSO with respect to the N_{amine} atoms (solid lines, left axis) and running coordination number cn(r) (dashed line, right axis). Each amine group is engaged in a N–H···O hydrogen bond with one DMSO molecule.

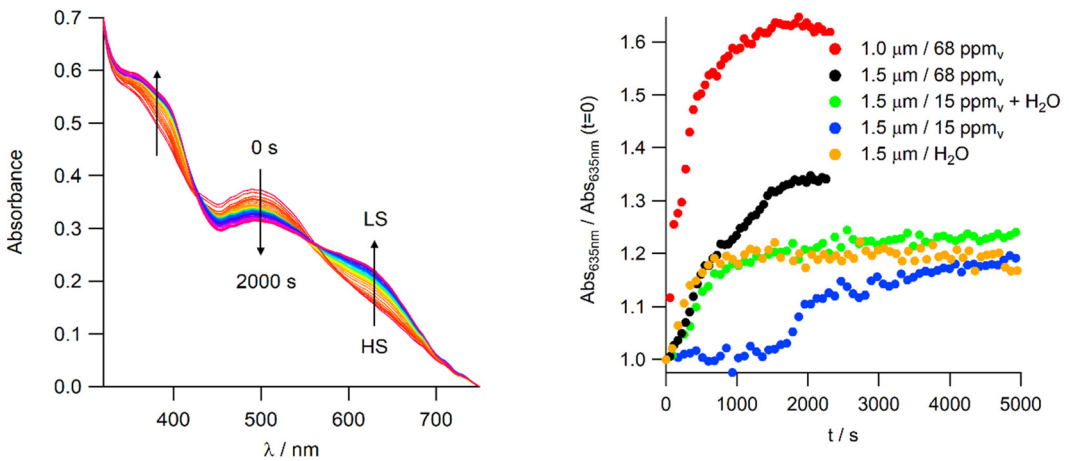

Fig. 3 (left) Evolution of the absorption spectrum of a 1.5 µm thick $Fe(Sal_2trien)NO_3$⊂MOF-808 film exposed to 68 ppm_v DMSO vapors; (right) evolution of the normalized absorption at 635 nm (corresponding to the LS absorption band) for several films/vapor compositions.

gas flow: 1.2 L min^{-1}, bubbler temperature: 30 °C) for 1 h at room temperature. Fig. 3 illustrates the evolution of the film absorbance during the exposure. A gradual increase in the bands at 630 nm, correlated to a decrease in the absorption at 500 nm, indicated a DMSO-induced HS-LS spin transition. The evolution of the absorbance at 630 nm, corrected from baseline fluctuation, is presented in Fig. 3. It evidences that the HS–LS transition follows single exponential kinetics with a half-time of 970 s. The same film was also investigated at a lower concentration of DMSO vapor (15 ppm_v) in order to investigate its sensitivity. Prior to the exposure to the lower concentration, the film was heated to 100 °C to remove the absorbed DMSO molecules. A similar HS–LS transformation was observed, although it was slower and less complete com-

pared to that obtained in the experiment performed with 68 ppm_v of DMSO (see Table 1 and Fig. S13).

The desorption process of DMSO was investigated to assess the reversibility of the sensing process. The chamber was flushed with solely N_2 at 400 mL min^{-1} at room temperature overnight to remove absorbed DMSO. A progressive recovery of the HS fraction was observed, suggesting a LS-to-HS transition (Fig. S14). However, the desorption process is not complete at room temperature, as the band at 630 nm (LS) remains visible after 9 h of N_2 flushing. This can be attributed to the inefficient removal of DMSO vapors from the chamber under N_2 flux at room temperature. We then subjected the film to a 100 °C heat treatment and showed that it led to a complete desorption of DMSO. Therefore, the same piece of the film was used for several consecutive measurements without any alteration of their switching properties. This reversibility indicates that the DMSO sensing mechanism is based on physisorption and that the thermal treatment effectively removes adsorbed DMSO and restores the switching state of the film, which highlights its potential for practical applicability as a reusable colorimetric sensor.

In order to explain the sensing potential of our films under environmental conditions, we then explored the influence of humidity on DMSO sensing. For such purposes, we first recorded the evolution of the film absorption in the presence of water vapor (>1000 ppm_v). A fast but partial HS–LS conversion was observed, which is consistent with magnetic measurements performed on powder (see Fig. S15). Therefore, the HS-LS conversion is by far more quantitative in the presence of 68 ppm_v of DMSO than with a large excess of water vapor (concentration >1000 ppm_v), which evidences the potential of the films for DMSO sensing in humid environments.

To investigate the competition between DMSO and water sorption, an experiment with a 15 ppm_v DMSO vapor concentration generated with a wet N_2 gas flux was performed. In this case, the HS–LS conversion was close to that observed in the presence of water vapor only, but slight differences appear after 1500 s of exposure (Fig. 3). Over this long exposure period, an additional slow HS–LS switching was observed, which is attributed to the slow kinetics of DMSO sorption into MOF-808 pores compared to water. This measurement evidenced that DMSO sensing can be performed even in the presence of water vapor down to 15 ppm_v, which is a prerequisite for the design of a colorimetric chemosensor.

Table 1 Kinetic parameters associated with the spin state switching of $Fe(Sal_2trien)NO_3$⊂MOF-808 films upon DMSO sorption

Film thickness	DMSO vapor concentration	Water vapor	$t_{1/2}$/s	Relative absorbance variation at 635 nm/%
1.5 μm	68 ppm_v	No	970	42
	15 ppm_v	No	2000	25
	15 ppm_v	Yes	710	25
	—	Yes	273	22
1.0 μm	68 ppm_v	No	320	58

Finally, we investigated the influence of film thickness on the spin state switching. With a thinner film (around 1.0 μm), the spin state switching occurred faster (320 s *vs.* 970 s) and with a higher relative amplitude (58% of relative variation of the optical density at 635 nm *vs.* 42%) compared to the 1.5 μm film. This observation was consistent with faster vapor diffusion kinetics in the thinner film. However, the absolute optical density variation at 635 nm is lower for the thinner film (see Fig. S13), which highlights the need to balance switching kinetics with the intensity of the color change when designing a colorimetric sensor. Overall, the sensitivity of these films compares well with that of previously reported spin crossover based porous solids.[17]

Conclusion

In this work, we have presented a convenient method to prepare a switchable $Fe(Sal_2trien)NO_3$⊂MOF-808 film of high optical quality and demonstrated its application as a DMSO colorimetric sensor. The color change observed upon DMSO vapor sorption is due to a HS-to-LS spin state switching of the $Fe(Sal_2trien)NO_3$ complexes loaded in MOF-808. This transition can be detected even at DMSO concentrations as low as 15 ppm_v and even in the presence of water vapor. Future work will be dedicated to the engineering of the MOF/spin crossover complex combination in order to design more selective and highly sensitive VOC colorimetric sensors. In a broader perspective, switchable porous solids based on the SCO⊂MOF compounds may also be used for the sensing of other pollutants such as CO_2, NO_x or SO_x.

Conflicts of interest

There are no conflicts to declare.

Data availability

The data supporting this article have been included as part of the supplementary information (SI). Supplementary information is available. See DOI: https://doi.org/10.1039/d5dt02285a.

Acknowledgements

A. T. thanks the ANR MOFSCO (ANR-18-CE09-0005-01) for funding the project. Y. S. thanks the UptoParis European Union's Horizon 2020 Research and Innovation program under the Marie Skłodowska-Curie grant agreement no. 754387. L. M. L. D. acknowledges grants from the Swiss National Supercomputing Centre (CSCS) under project IDs s894 and s1072, and supercomputing time from the Baobab HPC service of the University of Geneva.

References

1 A. J. Li, V. K. Pal and K. Kannan, A Review of Environmental Occurrence, Toxicity, Biotransformation and Biomonitoring of Volatile Organic Compounds, *Environ. Chem. Ecotoxicol.*, 2021, **3**, 91–116, DOI: 10.1016/j.enceco.2021.01.001.

2 X. Zhou, S. Lee, Z. Xu and J. Yoon, Recent Progress on the Development of Chemosensors for Gases, *Chem. Rev.*, 2015, **115**(15), 7944–8000, DOI: 10.1021/cr500567r.

3 M. Khatib and H. Haick, Sensors for Volatile Organic Compounds, *ACS Nano*, 2022, **16**(5), 7080–7115, DOI: 10.1021/acsnano.1c10827.

4 A. Azzouz, K. Vikrant, K.-H. Kim, E. Ballesteros, T. Rhadfi and A. K. Malik, Advances in Colorimetric and Optical Sensing for Gaseous Volatile Organic Compounds, *TrAC, Trends Anal. Chem.*, 2019, **118**, 502–516, DOI: 10.1016/j.trac.2019.06.017.

5 B. Siu, A. R. Chowdhury, Z. Yan, S. M. Humphrey and T. Hutter, Selective Adsorption of Volatile Organic Compounds in Metal-Organic Frameworks (MOFs), *Coord. Chem. Rev.*, 2023, **485**, 215119, DOI: 10.1016/j.ccr.2023.215119.

6 Y. Jin, H. Liu, M. Feng, Q. Ma and B. Wang, Metal–Organic Frameworks for Air Pollution Purification and Detection, *Adv. Funct. Mater.*, 2024, **34**(43), 2304773, DOI: 10.1002/adfm.202304773.

7 L. E. Kreno, K. Leong, O. K. Farha, M. Allendorf, R. P. Van Duyne and J. T. Hupp, Metal–Organic Framework Materials as Chemical Sensors, *Chem. Rev.*, 2012, **112**(2), 1105–1125, DOI: 10.1021/cr200324t.

8 F.-Y. Yi, D. Chen, M.-K. Wu, L. Han and H.-L. Jiang, Chemical Sensors Based on Metal-Organic Frameworks, *ChemPlusChem*, 2016, **81**(8), 675–690, DOI: 10.1002/cplu.201600137.

9 X. Wang, Y. Jiang, A. Tissot and C. Serre, Luminescent Sensing Platforms Based on Lanthanide Metal-Organic Frameworks: Current Strategies and Perspectives, *Coord. Chem. Rev.*, 2023, **497**, 215454, DOI: 10.1016/j.ccr.2023.215454.

10 Y. Shen, A. Tissot and C. Serre, Recent Progress on MOF-Based Optical Sensors for VOC Sensing, *Chem. Sci.*, 2022, **13**(47), 13978–14007, DOI: 10.1039/D2SC04314A.

11 Z. Chi, S. Chu, B. Wang, Z. Zhang, G. Liu and X. Wang, Advances in Metal Complex-Based Colorimetric Sensors, *Talanta*, 2026, **297**, 128591, DOI: 10.1016/j.talanta.2025.128591.

12 A. Tissot, X. Kesse, S. Giannopoulou, I. Stenger, L. Binet, E. Rivière and C. Serre, A Spin Crossover Porous Hybrid Architecture for Potential Sensing Applications, *Chem. Commun.*, 2019, **55**(2), 194–197, DOI: 10.1039/C8CC07573E.

13 S.-L. Yang, X. Zhang, Q. Wang, C. Wu, H. Liu, D. Jiang, R. Lavendomme, D. Zhang and E.-Q. Gao, Confinement inside MOFs Enables Guest-Modulated Spin Crossover of Otherwise Low-Spin Coordination Cages, *JACS Au*, 2023, **3**(8), 2183–2191, DOI: 10.1021/jacsau.3c00243.

14 P. Gütlich, A. B. Gaspar and Y. Garcia, Spin State Switching in Iron Coordination Compounds, *Beilstein J. Org. Chem.*, 2013, **9**, 342–391, DOI: 10.3762/bjoc.9.39.

15 E. Resines-Urien, E. Fernandez-Bartolome, A. Martinez-Martinez, A. Gamonal, L. Piñeiro-López and J. S. Costa, Vapochromic Effect in Switchable Molecular-Based Spin Crossover Compounds, *Chem. Soc. Rev.*, 2023, **52**(2), 705–727, DOI: 10.1039/D2CS00790H.

16 F. Moreau, J. Marrot, F. Banse, C. Serre and A. Tissot, Sequential Installation of Fe(ii) Complexes in MOFs: Towards the Design of Solvatochromic Porous Solids, *J. Mater. Chem. C*, 2020, **8**(47), 16826–16833, DOI: 10.1039/D0TC03756G.

17 E. Cuza, G. Patriarche, C. Serre and A. Tissot, New Architecture Based on Metal–Organic Frameworks and Spin Crossover Complexes to Detect Volatile Organic Compounds, *Chem. – Eur. J.*, 2024, **30**(38), e202400463, DOI: 10.1002/chem.202400463.

18 Y. Shen, J. Woodburn, S. Bouras, S. Dai, I. Dovgaliuk, J.-M. Grenèche, G. Patriarche, L. M. Lawson Daku, C. Serre and A. Tissot, Room-Temperature Bistability in Spin Crossover-Loaded Metal–Organic Frameworks, *Chem. Mater.*, 2023, **35**, 719–727, DOI: 10.1021/acs.chemmater.2c03426.

19 S. Dai, C. Simms, I. Dovgaliuk, G. Patriarche, A. Tissot, T. N. Parac-Vogt and C. Serre, Monodispersed MOF-808 Nanocrystals Synthesized via a Scalable Room-Temperature Approach for Efficient Heterogeneous Peptide Bond Hydrolysis, *Chem. Mater.*, 2021, **33**(17), 7054–7066, DOI: 10.1021/acs.chemmater.1c02174.

20 M. F. Tweedle and L. J. Wilson, Variable Spin Iron(111) Chelates with Hexadentate Ligands Derived from Triethylenetetramine and Various Salicylaldehydes. Synthesis, Characterization, and Solution State Studies of a New 2T-6A Spin Equilibrium System, *J. Am. Chem. Soc.*, 1976, **98**, 4824–4834.

21 K. Takeda, M. Pokorski, Y. Sato, Y. Oyamada and Y. Okada, Respiratory Toxicity of Dimethyl Sulfoxide, in *Respirology*, ed. M. Pokorski, Advances in Experimental Medicine and Biology, Springer International Publishing, Cham, 2015, vol. 885, pp. 89–96. DOI: 10.1007/5584_2015_187.

22 M. Verheijen, M. Lienhard, Y. Schrooders, O. Clayton, R. Nudischer, S. Boerno, B. Timmermann, N. Selevsek, R. Schlapbach, H. Gmuender, S. Gotta, J. Geraedts, R. Herwig, J. Kleinjans and F. Caiment, DMSO Induces Drastic Changes in Human Cellular Processes and Epigenetic Landscape in Vitro, *Sci. Rep.*, 2019, **9**(1), 4641, DOI: 10.1038/s41598-019-40660-0.